SELF-HEALING GOLD MIRRORS AND FILTERS AT LIQUID-LIQUID INTERFACES

Evgeny Smirnov, [1] Pekka Peljo, [1] Micheál D. Scanlon,[2] Frederic Gumy[1] and Hubert H. Girault[1,*]

[1] Laboratoire d'Electrochimie Physique et Analytique, Ecole Polytechnique Fédérale de Lausanne, Rue de l'Industrie 17, CH-1951 Sion, Switzerland.

[2] Department of Chemistry, the Tyndall National Institute and the Analytical & Biological Chemistry Research Facility (ABCRF), University College Cork, Cork, Ireland.

Table of Contents

Description	Page
SI-1: Optical microscopy and SEM observations of gold nanofilm formation step-by-step.	S3
SI-2: Interfacial surface tension measurements by a pendant drop method.	S5
SI-3: Comparison of the interfacial gold nanofilms formed with TTF at various water-organic solvent interfaces	S7
SI-4: Influence of the interfacial surface tension on the interfacial gold nanofilm's luster.	S8
SI-5: Comparison of interfacial gold nanofilms formed on varying the nature of the lipophilic molecule dissolved in the oil droplet.	S10
SI-6: Supplementary references.	S11

SI-1. Optical microscopy and SEM observations of gold nanofilm formation step-by-step

An *in situ* optical microscopy investigation, with *ex situ* SEM images, of the interfacial gold nanofilms formed with 38 nm mean diameter (Ø) AuNPs at a water-DCE interface was performed in order to show the morphological changes of the interfacial gold nanofilm during the systematic increase of the interfacial AuNP surface coverage nanofilm (θ_{int}^{AuNP}), see Fig. S1.

At low θ_{int}^{AuNP}, such as at 0.1 and 0.2 monolayers (MLs, the definition of the dimensionless ML term is given in the main text), the AuNPs were organized in low-density "floating AuNP islands". Some of the latter were interconnected, whereas others were separated and independent, see Fig. S1A & B. Then, at a θ_{int}^{AuNP} of 0.4 ML, the AuNPs filled the majority of the available surface area at the interface, eliminating any large voids in between the AuNP clusters on the micron scale. However, small voids were still seen, especially in SEM images (Fig. S1C).

At a θ_{int}^{AuNP} of 0.6-0.8 ML, the density of the interfacial gold nanofilms increased markedly (Fig. S1D & E). Significant numbers of cracks were seen on both the *in situ* optical and *ex situ* SEM images, perhaps indicative of the continuous rearrangement and increase in packing densities of the AuNPs in the interfacial nanofilms at these values of θ_{int}^{AuNP}. Despite this, it should be noted that the interfacial gold nanofilm in Fig. S1E is not extremely dense, being 20% below the maximum value of θ_{int}^{AuNP} theoretically attainable by a hexagonally close-packed arrangement. The morphology of these interfacial gold nanofilms, shown in Fig. S1D & E, possessed the maximum values for reflectance, as shown in Fig. 2 in the main text and discussed in detail therein.

Beyond sub-monolayer conditions, with θ_{int}^{AuNP} of 1.0 and 2.0 ML Fig. S1F & G, large horizontally stretched dark lines, perhaps representation of wrinkles in the interfacial gold nanofilms due to buckling at the interface, were observed in the optical images. The SEM images at these high AuNP surface coverages clearly show a huge proliferation of piles of AuNPs on top of the underlying 2D monolayer of AuNPs adsorbed at the interfaces. Both the macroscale effect

of wrinkling and the nanoscale effect of 3D nanostructuring of the interface lead to a significant loss of reflectance, as shown in Fig. 2 in the main text.
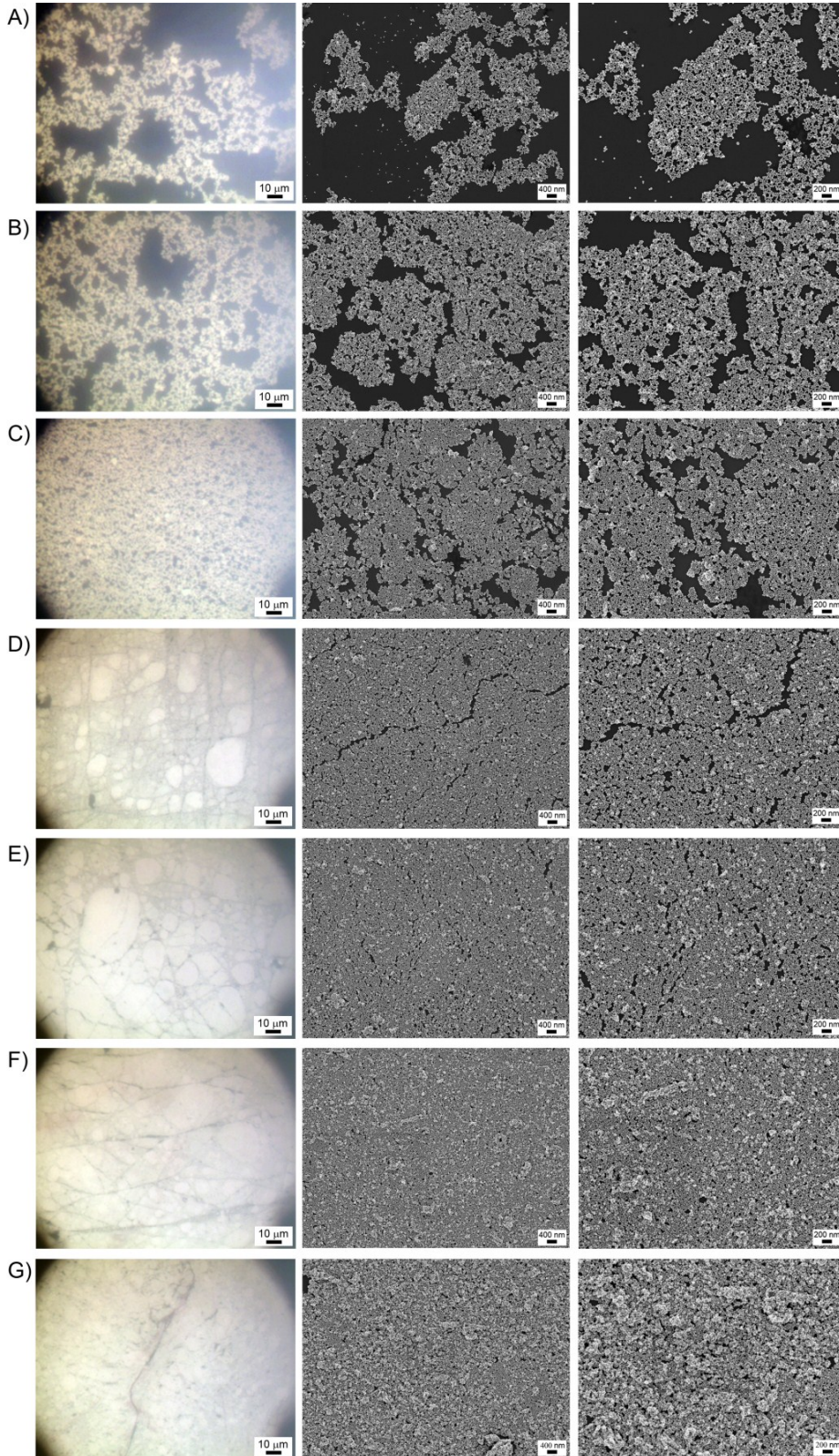

Figure S1. Comparison of optical microscopy images (50x magnification) performed in situ and ex situ SEM images of the interfacial gold nanofilms transferred to a silicon substrate. The coverages of the interface (θ_{int}^{AuNP}) in monolayer are as following: **(A)** 0.1 ML, **(B)** 0.2 ML, **(C)** 0.4 ML, **(D)** 0.6 ML, **(E)** 0.8 ML, **(F)** 1.0 ML, and **(G)** 2.0 ML. Scales bars are from left to right 10 μm, 400 nm and 200 nm.

SI-2. Interfacial surface tension measurements by a pendant drop method

Pendant drop measurements were carried out on a drop shape analysis system DSA100 (Kruss, Germany). All glassware used was cleaned with a mixture of nitric and hydrochloric acid (*aqua regia*), washed several times with pure water, dried and then treated with oxygen plasma for 30 minutes in order to eliminate any presence of other compounds. Each organic solution was vigorously shaken with Milli-Q water and subsequently the biphasic system was left overnight in order to obtain saturated solutions (aqueous with organic phase and organic with aqueous phase, respectively).
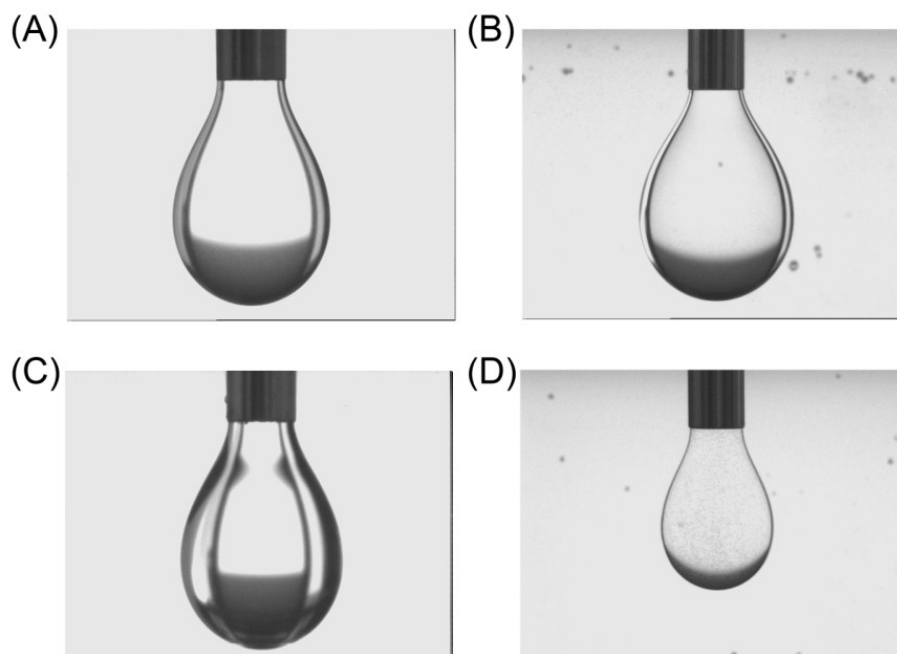

Figure S2. Pendant drop measurements of the interfacial surface tension($\gamma_{w/o}$) for each biphasic system studied: (A) water-1,2-dichloroethane (DCE), **(B)** water-α,α,α,-trifluorotoluene (TFT), **(C)** water-nitrobenzene (NB) and **(D)** water-nitromethane (MeNO$_2$) systems.

Based on shapes of the obtained pendant drops and physical properties of the solvents used, values for the interfacial tension were calculated as follows:

- γ(w-DCE) = 30.5±0.3 mN·m^{-1}. This value corroborates with the value of 28 mN·m^{-1} reported previously.[1,2]

- γ(w-TFT) = 38.0±0.5 mN·m^{-1}. This value is close to that reported for water | toluene biphasic systems as predicted by Bahramian *et al.*[3] To the best knowledge of our knowledge, no previous work has measured a value of γ(w-TFT).

- γ(w-NB) = 24.4±0.2 mN·m^{-1}.

- γ(w-MeNO$_2$) = 16.0±0.2 mN·m^{-1}. For MeNO$_2$ the value is slightly higher than that predicted by Bahramian *et al.*[3].

SI-3. Comparison of the interfacial gold nanofilms formed with TTF at various water-organic solvent interfaces
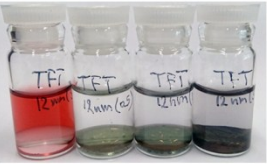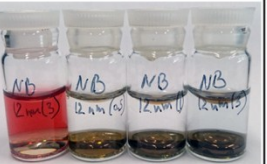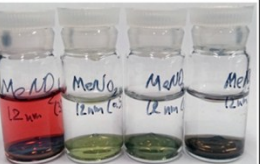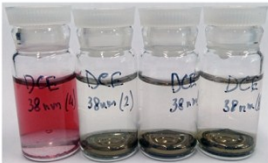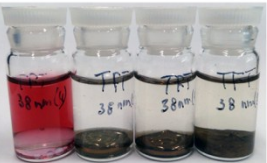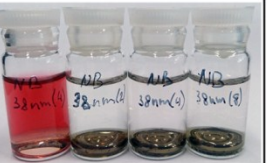

Figure S3. Optical photographs of interfacial gold nanofilms formed at water-DCE, water-TFT, water-NB and water-MeNO₂ interfaces prepared with AuNPs of either 12 or 38 nm Ø. The Numbers under each picture display θ_{int}^{AuNP} value in each case.

SI-4. Influence of the interfacial surface tension on the interfacial gold nanofilm's luster

(A)

(B)

(C) DCE

(D) TFT

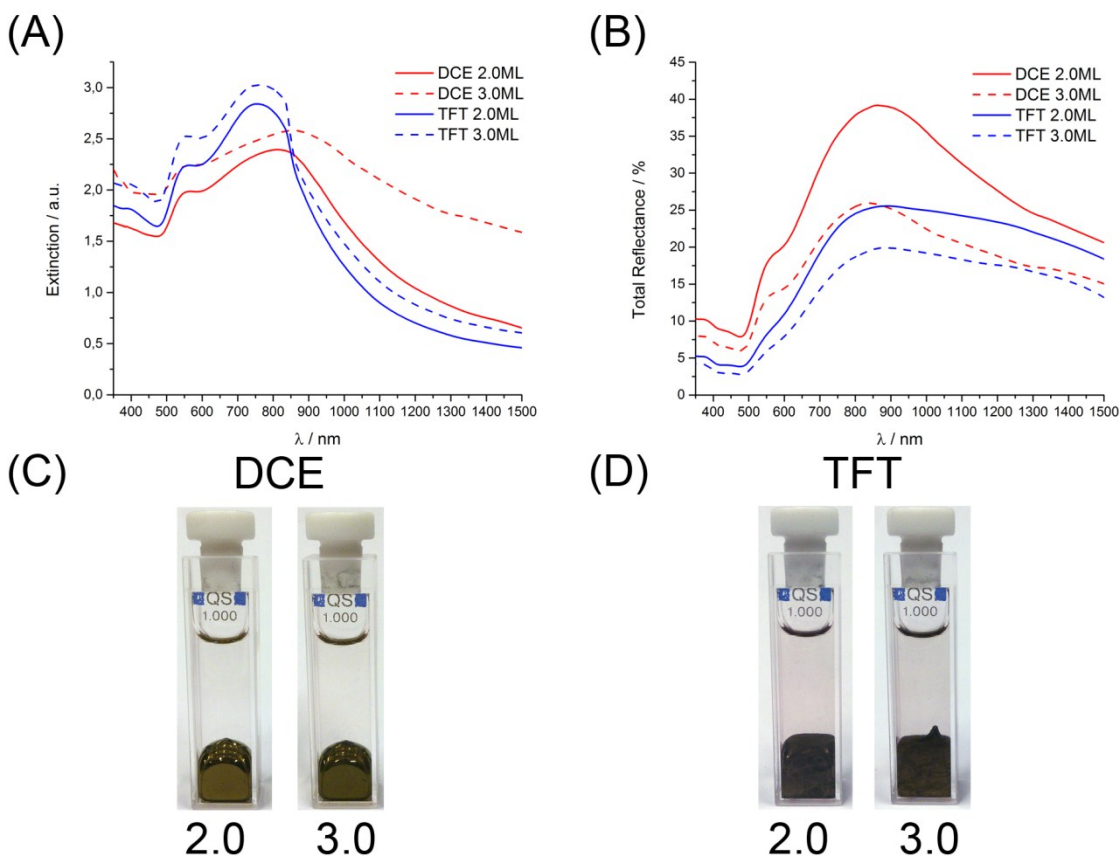**Figure S4. Influence of the interfacial tension on optical responses from interfacial gold nanofilms: (A)** Extinction and (**B**) total reflectance spectra for interfacial gold nanofilms prepared with 38 nm Ø AuNPs at water-DCE and water-TFT interfaces. **(C, D)** Optical photographs of the obtained nanofilms at water-DCE and water-TFT interfaces at $\theta_{\text{int}}^{\text{AuNP}}$ value of 2.0 and 3.0 ML, respectively.

There are several types of interactions between NPs at liquid-liquid interfaces: capillary, electrostatic, Van der Waals, fluctuation and solvation.[6,7] However, only a few of them, namely capillary and electrostatic forces, are strong enough to have a significant effect on relatively large NPs. Herein, we show that AuNPs may be assembled in closed-packed arrays of particles,

meaning that the electrostatic interactions between separate AuNPs are significantly minimized in comparison to colloidal citrate stabilized solutions of AuNPs, for example.[8] Thus, the main force acting at the liquid-liquid interface and affecting the assembly of the AuNPs is a capillary immersion force. According to Bresme's review[6] and the work of Kralchevsky and Nagayama[7], this capillary interaction may be defines as:

$$U_{cap} \propto \gamma_{w/o} R^2 K_0(qd) \xrightarrow{qd=1} -\gamma_{w/o} R^2 \ln(qd) \tag{1}$$

where is the interfacial tension, $K_0(qd)$ is the modified Bessel function of zeroth order, d is the distance between particles, q is the inverse capillary length in thin film. This equation is valid when d is much smaller than q (order of several nm^{-1}) and when the radii of the two contact lines is much smaller that the particle separation.[6] Also, q is determined as:

$$q = \sqrt{(\Delta\rho g - \Pi')/\gamma_{w/o}} \tag{2}$$

where Π' is the derivative of the disjoining pressure with respect to the film thickness. Thus, the interfacial tension should have a major effect on interfacial gold nanofilms, causing a stronger capillary interaction between the AuNPs.

The interfacial surface tension for a water-TFT interface was determined as ~25% higher than that for a water-DCE interface (38 *vs* 30 mN/m, respectively), as shown *vide supra*. Thus, this higher interfacial surface tension at water-TFT interfaces results in stronger capillary interactions causing the formation of deep and large buckles and wrinkles. As a consequence, this directly leads to an increase in the scattering and subsequent absorption of the incident light for these interfacial gold nanofilms formed at high surface coverages. This effect is clearly shown in Fig. S4A & B and leads to significant increases in extinction and decreases in reflectance in comparison to interfacial gold nanofilms formed at water-DCE interfaces under otherwise identical experimental conditions. The lower interfacial tension of the latter is not strong enough to significantly buckle the interfacial gold nanofilms, keeping them relatively flat at the interface even at high surface coverages. The major changes in extinction and reflection profiles between the interfacial gold nanofilms formed at each water-organic solvent interface are clearly evident in the optical photographs shown in Fig. S4C & D: gold/yellow and shiny nanofilms at water-DCE interfaces and much dimmer gold nanofilms with no luster at water-TFT interfaces.

SI-5. Comparison of interfacial gold nanofilms formed on varying the nature of the lipophilic molecule dissolved in the oil droplet
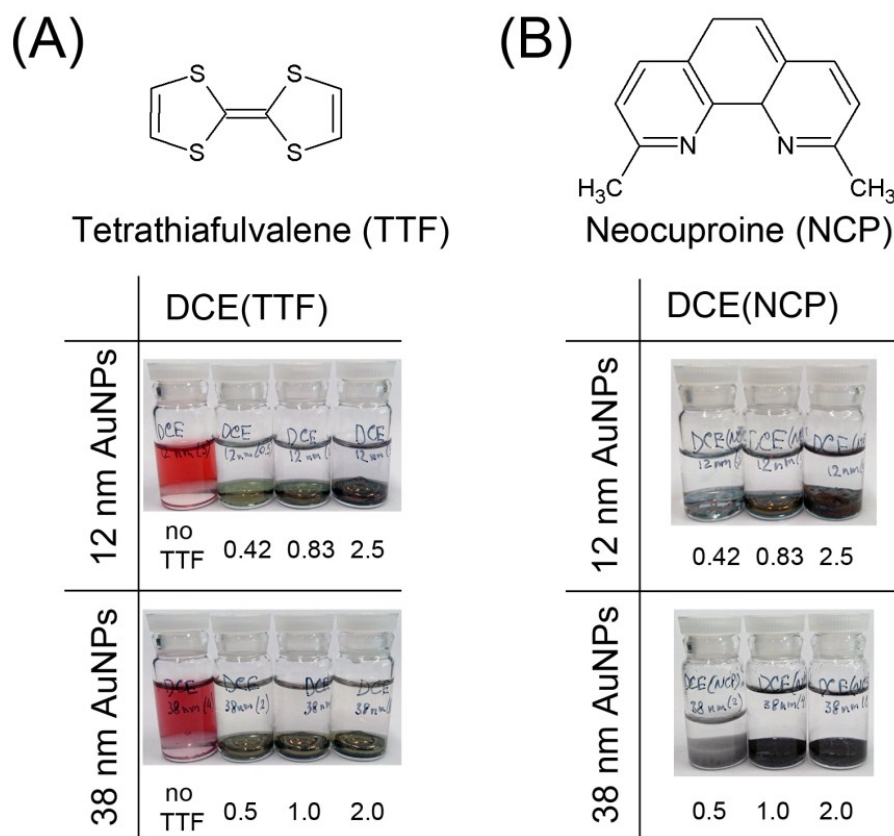

Figure S5. Optical photographs of interfacial gold nanofilms at water-DCE interfaces prepared with (A) tetrathiafulvalene (TTF) and (B) neocuproine (NCP) molecules dissolved in the oil droplet. The nanofilms formed with both 12 and 38 nm Ø AuNPs are shown. The numbers under each picture display the $\theta_{\text{int}}^{\text{AuNP}}$ value.

Neocuproine (NCP) molecules has previously been shown to promote the self-assembly of silver NPs into lustrous nanofilms.[4,5] The structures of TTF and NCP molecules are given in Fig. S5. When NCP was dissolved in the DCE droplet, only those interfacial gold nanofilms formed with 12 nm Ø AuNPs exhibited similar optical responses to TTF-based assemblies. Meanwhile, with NCP, 38 nm Ø AuNPs formed black nanofilms, the origin of which is the variation of the interparticle distance on changing the ligand around the AuNPs in the interfacial gold nanofilm. NCP allows the AuNPs to approach closer to each other in the nanofilm, leading to strong interparticle plasmon coupling and a broadband absorbance, as clearly shown in Fig. 6 in the main text and discussed in detail therein.

SI-6. Supplementary references:

(1) Girault, H. H. J.; Schiffrin, D. J. Adsorption of Phosphatidylcholine and Phosphatidyl-Ethanolamine at the Polarised water/1,2-Dichloroethane Interface. *J. Electroanal. Chem. Interfacial Electrochem.* **1984**, *179*, 277–284.

(2) Kakiuchi, T.; Nakanishi, M.; Senda, M. Electrocapillary Curves of the Phosphatidylcholine Monolayer at the Polarized Oil–water Interface. I. Measurement of Interfacial Tension Using a Computer-Aided. *Bull. Chem. Soc. Japan* **1988**, *61*, 1845–1851.

(3) Bahramian, A.; Danesh, A. Prediction of Liquid–liquid Interfacial Tension in Multi-Component Systems. *Fluid Phase Equilib.* **2004**, *221*, 197–205.

(4) Gingras, J.; Déry, J.-P.; Yockell-Lelièvre, H.; Borra, E. F.; Ritcey, A. M. Surface Films of Silver Nanoparticles for New Liquid Mirrors. *Colloids Surfaces A Physicochem. Eng. Asp.* **2006**, *279*, 79–86.

(5) Yen, Y.; Lu, T.; Lee, Y.; Yu, C.; Tsai, Y.; Tseng, Y.; Chen, H. Highly Reflective Liquid Mirrors: Exploring the Effects of Localized Surface Plasmon Resonance and the Arrangement of Nanoparticles on Metal Liquid-like Films. *ACS Appl. Mater. Interfaces* **2014**, *6*, 4292–4300.

(6) Bresme, F.; Oettel, M. Nanoparticles at Fluid Interfaces. *J. Phys. Condens. Matter* **2007**, *19*, 413101.

(7) Kralchevsky, P. A.; Nagayama, K. Capillary Interactions between Particles Bound to Interfaces, Liquid Films and Biomembranes. *Adv. Colloid Interface Sci.* **2000**, *85*, 145–192.

(8) Smirnov, E.; Scanlon, M. D.; Momotenko, D.; Vrubel, H.; Méndez, M. a; Brevet, P.-F.; Girault, H. H. Gold Metal Liquid-like Droplets. *ACS Nano* **2014**, *8*, 9471–9481.